Adenosine Triphosphate-Induced Electron Transfer in 2-Hydroxyglutaryl-CoA Dehydratase from *Acidaminococcus fermentans*†

Marcus Hans,‡,§ Eckhard Bill,|| Irina Cirpus,‡ Antonio J. Pierik,‡ Marc Hetzel,‡ Dorothea Alber,⊥ and Wolfgang Buckel*,‡

Laboratorium für Mikrobiologie, Fachbereich Biologie, Philipps-Universität, Marburg, Germany, Max-Planck Institut für Strahlenchemie, Mülheim an der Ruhr, Germany, and Hahn-Meitner-Institut Berlin, Germany

Received January 14, 2002

ABSTRACT: 2-Hydroxyglutaryl-CoA dehydratase from *Acidaminococcus fermentans* catalyzes the chemical difficult elimination of water from (*R*)-2-hydroxyglutaryl-CoA to glutaconyl-CoA. The enzyme consists of two oxygen-sensitive protein components, the homodimeric activator (A) with one [4Fe-4S]$^{1+/2+}$ cluster and the heterodimeric dehydratase (D) with one nonreducible [4Fe-4S]$^{2+}$ cluster and reduced riboflavin 5′-monophosphate ($FMNH_2$). For activation, ATP, Mg^{2+}, and a reduced flavodoxin (16 kDa) purified from *A. fermentans* are required. The [4Fe-4S]$^{1+/2+}$ cluster of component A is exposed to the solvent since it is accessible to iron chelators. Upon exchange of the bound ADP by ATP, the chelation rate is 8-fold enhanced, indicating a large conformational change. Oxidized component A exhibits ATPase activity of 6 s^{-1}, which is completely abolished upon reduction by one electron. UV−visible spectroscopy revealed a spontaneous one-electron transfer from flavodoxin hydroquinone ($E_0' = -430$ mV) to oxidized component A, whereby the [4Fe-4S]$^{2+}$ cluster of component A became reduced. Combined kinetic, EPR, and Mössbauer spectrocopic investigations exhibited an ATP-dependent oxidation of component A by component D. Whereas the [4Fe-4S]$^{2+}$ cluster of component D remained in the oxidized state, a new EPR signal became visible attributed to a d^1-metal species, probably Mo(V). Metal analysis with neutron activation and atomic absorption spectroscopy gave 0.07−0.2 Mo per component D. In summary, the data suggest that in the presence of ATP one electron is transferred from flavodoxin hydroquinone via the [4Fe-4S]$^{1+/2+}$ cluster of component A to Mo(VI) of component D, which is thereby reduced to Mo(V). The latter may supply the electron necessary for transient charge reversal in the unusual dehydration.

2-Hydroxyglutaryl-CoA dehydratase from *Acidaminococcus fermentans* (order Clostridiales) catalyzes the reversible *syn*-elimination of water from (*R*)-2-hydroxyglutaryl-CoA to (*E*)-glutaconyl-CoA (*1*) as depicted in Scheme 1 (*2*). This reaction is the key step of the '2-hydroxyglutarate pathway', by which glutamate is fermented to ammonia, carbon dioxide, acetate, butyrate, and molecular hydrogen (*3*−*5*). The dehydratase consists of two proteins: the extremely oxygen-sensitive homodimeric component A (HgdC, γ_2, 2 × 27 kDa), an activating or initiating protein; and the moderate oxygen-sensitive heterodimeric component D (HgdAB, $\alpha\beta$, 50 + 45 kDa), which most likely harbors the substrate binding site (*2*, *6*, *7*). To obtain activity, the substrate, both components, Mg^{2+}, catalytic amounts of ATP, and a reducing agent such as titanium(III) citrate or dithionite are required (*8*). Each component contains 1.0 mol of [4Fe-4S] cluster; component D possesses in addition FMN[1] hydroquinone (1.0 mol) and trace amounts of riboflavin (<0.1 mol). Whereas the diamagnetic [4Fe-4S]$^{2+}$ cluster of component A can be easily reduced with one electron, that of component D is resistant to the reducing agents mentioned above, even when applied in large excess. The paramagnetic [4Fe-4S]$^{+}$ cluster of the reduced component A exhibits the unusual electron spin ground state $S = 3/2$ as indicated by strong absorption-type EPR signals at high g values, $g = 4-6$ (*7*). The structure of component A has been determined by X-ray crystallography at 3 Å resolution. It confirmed the biochemical data of a homodimeric protein with a bridging [4Fe-4S] cluster and an ATP binding site in each subunit, which is occupied by ADP. The [4Fe-4S] cluster is located between the *N*-termini of two helices, with helix 5 of each subunit called the 'cluster helix'. The angle helix−[4Fe-4S]−helix is about 105° (*9*). The probably functionally related nitrogenase iron protein also contains this arrangement (or novel prosthetic group) composed of a helix from each subunit bridged by a [4Fe-4S] cluster, but the angle (150°) is substantially larger (*10*).

† This work was supported by grants from the Deutsche Forschungsgemeinschaft (DFG) and the Fonds der Chemischen Industrie.

* Correspondence should be addressed to this author at the Laboratorium für Mikrobiologie, Fachbereich Biologie, Philipps-Universität, D-35032 Marburg, Germany. Fax: +49 6421 2828979, E-mail: Buckel@mailer.uni-marburg.de.

‡ Philipps-Universität.

§ Present address: Department of Chemistry and Chemical Engineering, Stauffer III, Stanford University, Stanford, CA 94305.

|| Max-Planck Institut für Strahlenchemie.

⊥ Hahn-Meitner-Institut Berlin.

[1] Abbreviations: AMP-PNP, adenosine 5′-(β,γ-iminotriphosphate); ATP, adenosine 5′-triphosphate; CoA, CoASH, coenzyme A; EPR, electron paramagnetic resonance; FMN, riboflavin 5′-phosphate; MALDI-TOF, matrix-assisted laser desorption ionization time-of-flight; Mops, morpholinopropanesulfonic acid; NADH, reduced form of nicotinamide adenine dinucleotide; thionine, 7-amino-3-imino-3*H*-phenothiazine; Tris, tris(hydroxymethyl)aminomethane. Enzymes: 2-Hydroxyglutaryl-CoA dehydratase (EC 4.2.1.-); nitrogenase (EC 1.18.6.1).

10.1021/bi020033m CCC: $22.00
Published on Web 04/11/2002

Scheme 1: Proposed Mechanism of the Reversible *syn*-Elimination of Water from (*R*)-2-Hydroxyglutaryl-CoA to (*E*)-Glutaconyl-CoA[a]

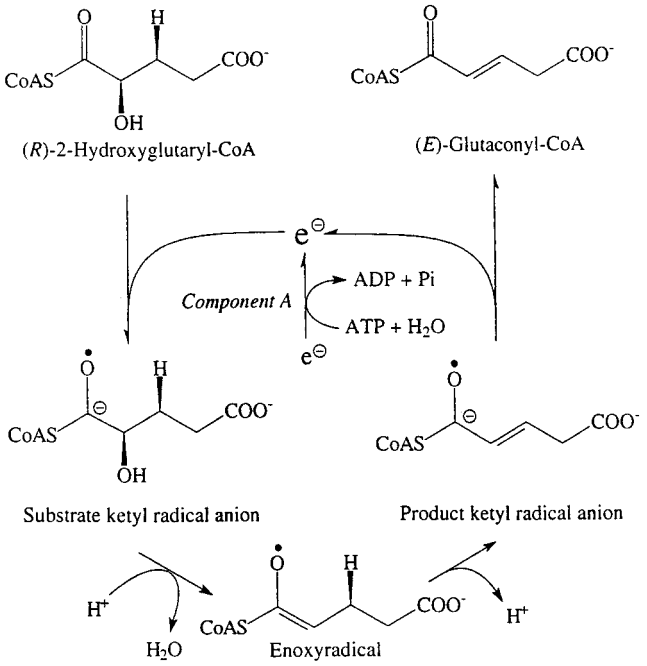

[a]Component A catalyzes the ATP-dependent electron transfer; the size of the 'e' indicates the energy content of the electron. All other reactions are catalyzed by component D.

In contrast to the dehydration of 3-hydroxyacyl thiol esters in fatty acid biosynthesis, in 2-hydroxyglutaryl-CoA the hydroxyl group occupies the 'wrong' α-position adjacent to the electron-withdrawing thiol ester carbonyl, and the hydrogen to be removed as proton sits in the nonactivated β-position. This unusual elimination requires a transient reversal of the positively charged thiol ester carbonyl to a negatively charged ketyl radical anion, which could be achieved by reduction with a low-potential electron (*11*). It has been postulated, therefore, that driven by ATP-hydrolysis component A introduces an electron into component D and further to the 2-hydroxyglutaryl-CoA. The nucleophilic ketyl radical anion eliminates the adjacent hydroxyl group to form an enoxy radical, which after deprotonation yields the ketyl radical anion of glutaconyl-CoA. Reoxidation to the product by the next incoming 2-hydroxyglutaryl-CoA completes the catalytic cycle. Therefore, only substoichiometric amounts of ATP are required to initiate the catalytic cycle for many turnovers (Scheme 1) (*2*, *12*). This paper describes isolation of a flavodoxin from cell-free extracts of *A. fermentans*, which in the hydroquinone form can replace the artificial electron donors in the initiation of the dehydration. The results demonstrate the postulated one-electron transfer from flavodoxin to component A. In the presence of ATP, the electron is further transferred to component D, which may supply the electron for the charge reversal.

MATERIALS AND METHODS

Materials. Morpholinepropanesulfonic acid (Mops) was purchased from Serva (Heidelberg, Germany). FPLC columns were obtained from Pharmacia LKB Biotechnology (Uppsala, Sweden). Streptavidin Sepharose and the plasmid pASK-IBA3 were from IBA-GmbH (Göttingen, Germany). ^{57}Fe metal was purchased from Chemotrade (Düsseldorf, Germany). The metal (25 mg) was dissolved in 0.5 mL of 7 M HCl at 80 °C. To prepare ^{57}Fe-enriched cells, 50 mL of this ^{57}Fe solution was added to 1 L of culture medium. No attempt was made to remove the ^{56}Fe present in the yeast extract of the medium. The protein molecular mass marker was from Roche (Mannheim, Germany). All other chemicals were from Sigma or Fluka (Deisenhofen, Germany).

Performance of Anaerobic Experiments. All buffers, media, and solutions were prepared anoxically by boiling for 5 min and cooling under vacuum. The buffers were transferred in gastight bottles into the anaerobic chamber (Coy Laboratories, Ann Arbor, MI), whose atmosphere consisted of 5% H_2 in 95% N_2. At this stage, heat-sensitive substances were added. Complete removal of molecular oxygen was achieved either by intensive stirring or by bubbling N_2 through the solutions. Dithionite was added at least 1 h before using the buffer in order to avoid reactive intermediates, which could interact with proteins. All protein purification steps and manipulations such as preparing and freezing EPR and Mössbauer samples were performed in the anaerobic chamber.

Synthesis of Oxygen-Free 2-Hydroxyglutaryl-CoA. Synthesis of (*R*)-2-hydroxyglutaryl-CoA was performed enzymatically by using recombinant glutaconate CoA-transferase from *A. fermentans* (*13*) under strictly anaerobic conditions. To a mixture of 50 μL of 38 mM acetyl-CoA and 200 μL of 250 mM (*R*)-2-hydroxyglutarate, sodium salt, pH 8, was added 40 mg of glutaconate CoA-transferase in 150 μL of 50 mM Tris/HCl, pH 8.0, 0.3 M NaCl, and 10 mM $MgCl_2$. After 5 min at room temperature, the CoA-transferase was removed by ultrafiltration with a centricon-filter YM30. The concentration of (*R*)-2-hydroxyglutaryl-CoA in the flow-through was determined by conversion to acetyl-CoA using glutaconate CoA-transferase and 100 mM acetate. Acetyl-CoA was quantified in an assay involving citrate synthase, oxaloacetate, and 5,5′-dithiobis(2-nitrobenzoate) using an absorbency coefficient, $\epsilon = 14.0\ mM^{-1}\ cm^{-1}$ (*14*, *15*).

Bacteria. *Acidaminococcus fermentans* ATCC 25085 was grown anaerobically on the sodium glutamate/yeast extract medium described earlier (*16*). For flavodoxin isolation, the bacteria were grown without added iron (1−2 μM iron mainly from the yeast extract). *Escherichia coli* strain XL1-blue MRF′ (Stratagene, Heidelberg, Germany) was grown on Standard I nutrient broth (Merck, Darmstadt, Germany) under anaerobic conditions (*7*). The strain was used for component A synthesis by expression of *hgdC* from *A. fermentans* (cloned in pASK-IBA3 to yield the plasmid pMH6, IBA-GmbH, Göttingen, Germany).

Spectroscopic Methods. Perpendicular as well as parallel mode X-band EPR spectra were recorded with a Bruker ESP 300E cw spectrometer, interfaced with an Oxford ESR910 liquid helium cryostat. A Bruker ER 4116 DM dual mode cavity was used to generate the microwave fields, H_1, parallel and perpendicular to the static field. All perpendicular mode spectra were recorded at 10 K, microwave power 20 mW ($[4Fe\text{-}4S]^+$ $S = 3/2$ spectra) or 0.1 mW ($[3Fe\text{-}4S]^+$ $S = 1/2$ spectra), microwave frequency 9.65 GHz, modulation amplitude 1.2−1.5 mT, and modulation frequency 100 kHz. The conditions for parallel mode EPR were temperature 10 K, microwave frequency 9.33 GHz, microwave power 20

mW, modulation amplitude 1.5 mT, and modulation frequency 50 kHz.

Mössbauer data were collected on an alternating constant-acceleration spectrometer. The sample temperature was maintained constant either in an Oxford Variox or in an Oxford Mössbauer-Spectromag cryostat. The latter is a split pair conducting magnet system for applying fields up to 8 T to the samples, which can be kept at temperatures in the range of 1.5−250 K. The field in the sample is perpendicular to the γ-beam. With the help of re-entrant bore tubes, the ^{57}Co/Rh source was positioned at room temperature inside the gap of the magnet system at a distance of about 85 mm from the sample. At this position, the magnetic field is zero. All isomer shifts are quoted relative to iron metal at 300 K.

The 80 K Mössbauer spectra of the ^{57}Fe-enriched component A preparations with ADP, ATP, and ATP + substrate (Figure 6A−C) were simultaneously fitted by using symmetric Lorentzian doublets. Only the absorption depths were allowed to vary within the series. The low-temperature spectra with applied field were simulated by using the spin-Hamiltonian formalism for $S = 3/2$ (reduced component A) or $S = 0$ (component D). For details, see (*7*).

UV−visible spectra were recorded on a Kontron UVIKON 910 double beam absorption spectrometer (Kontron, Heidelberg, Germany) with cuvettes sealed with gastight rubber stoppers.

Biochemical Methods. The protein concentrations were determined by using the Bio-Rad Microassay (*17*) or the Pierce BCA-Macroassay (*18*) with bovine serum albumin as standard. SDS−PAGE was performed in a Mini Protean apparatus from Bio-Rad (Heidelberg, Germany). Protein was stained with Coomassie Brillant Blue R-250 (Serva, Heidelberg, Germany). The activity of both 2-hydroxyglutaryl-CoA dehydratase components A and D was assayed using the coupled method described earlier (*8, 19*). Non-heme iron and acid-labile sulfide were determined as described previously (*20, 21*). The redox titration of the flavodoxin was performed using an Ingold Pt 4805-S7/120 platinum electrode combined with an Ag/AgCl reference electrode. The following mediator substances (10 μM each) were added to 50 μM flavodoxin in 20 mM Mops, pH 7.0: methyl viologen, benzyl viologen, anthraquinone-2-sulfonate, 2-hydroxy-1,4-naphthoquinone, menadione, 2-methyl-1,4-naphthoquinone. The formation and disappearance of flavodoxin semiquinone were monitored at $\lambda = 578$ nm. ATPase activity of component A was measured with a coupled enzyme assay using pyruvate kinase and lactate dehydrogenase. Component A (10 μL) was added to 50 mM Tris/HCl, pH 8.0, 0.2 mM NADH, 1 mM phosphoenolpyruvate, 5 mM ATP, 10 mM $MgCl_2$, 1 unit of pyruvate kinase, and 1 unit of lactate dehydrogenase in a total volume of 1.0 mL. The consumption of NADH was measured at $\lambda = 340$ nm.

Molybdenum was determined by atomic absorption spectroscopy (Perkin-Elmer) using $(NH_4)_6Mo_7O_{24}\cdot 4H_2O$ standards containing up to 500 pg (5.2 pmol) of Mo. The sample was preheated to 1800 °C and then measured at 2650 °C. The light source was a molybdenum lamp at $\lambda = 313.3$ nm. Molybdenum and tungsten were also determined by instrumental neutron activation analysis. The lyophilized protein samples were irradiated in the research reactor BERII of the Hahn-Meitner-Institut (Berlin, Germany) for 40 h at a flux of 1.3×10^{14} neutrons cm^{-2} s^{-1}. Elemental standards were obtained from Merck (Darmstadt, Germany). As quality control for the molybdenum determination, bovine liver was used (no. 1577b of the National Institute of Standards and Technology, Washington, DC).

Purification of Recombinant Component A. An overnight culture (25 mL) of recombinant *E. coli* (XL1-blue/pMH6) was used to inoculate five tightly closed 2 L bottles filled with Standard I medium under a N_2 atmosphere at 30 °C. When $OD_{600} = 0.3$ was reached, synthesis of recombinant component A (HgdC) was induced with anhydrotetracycline (30 mg/L). After anaerobic growth for a further 3 h, cells were harvested and suspended in buffer B containing 20 mM Mops, pH 7.2, 100 mM NaCl, 10 mM $MgCl_2$, 1 mM ATP, and 4 mM dithionite. The bacteria were broken using a French Press cell at 140 MPa, which was filled in the anaerobic chamber. The cell was inserted into the press, and the outlet was connected to an N_2-containing serum bottle by a silicon tube and a syringe needle through the rubber stopper of the bottle. Cell debris and membranes were removed by ultracentrifugation for 60 min at 100000*g*. The supernatant was loaded by gravity flow onto an 8 mL StrepTactin Sepharose column, which was equilibrated at 20 °C with the buffer described above. After complete binding, the column was washed with at least 10 column volumes buffer B. Component A was eluted with buffer B containing 2.5 mM D-desthiobiotin. The protein was concentrated by ultrafiltration in a stirred Amicon cell with a YM-30 filter and immediately used for further experiments (*22*). To determine the difference of the extinction coefficient of the reduced minus the oxidized form of component A, the protein was reduced with sodium dithionite or oxidized with thionine. After removal of excess reductant or oxidant by gel filtration on Sephadex G-25, the difference spectrum yielded $\Delta\epsilon_{400} = -4.5$ mM^{-1} cm^{-1}.

Purification of Component D. Wet cells (30 g) from *A. fermentans* were suspended in 80 mL of buffer A (20 mM Mops, pH 7.0; 2 mM dithiothreitol) and broken using a sonifier (Branson, Ultrasonics, Danbury, CT) at a power of 80 W under cooling with ice. After ultracentrifugation (100000*g*, 60 min at 4 °C), the supernatant was filtered (0.45 μm pore size) and loaded onto a DEAE-Sepharose fast-flow column (2.6 × 20 cm). Elution of component D with a linear NaCl gradient (0−1 M NaCl in 700 mL of buffer A) occurred at 0.3 M NaCl in a volume of 60 mL. After adjusting the pooled fractions to 1.0 M ammonium sulfate, the protein solution was loaded onto a phenyl-Sepharose fast-flow column equilibrated with 1 M ammonium sulfate in buffer A. The enzyme was eluted by a linear gradient of 1−0.3 M ammonium sulfate in 600 mL of buffer A. After desalting the active fractions by ultrafiltration (YM 10 filter, Amicon), chromatography on a Q-Sepharose high-performance column lead to homogeneous component D. The protein was eluted by applying a linear gradient of 0−0.7 M NaCl in 400 mL of buffer A. Component D is oxygen-sensitive and can be stored under anaerobic conditions at 4 °C for about 1 week without loss of activity.

Purification of Flavodoxin from A. fermentans. Initially the procedure was the same as that for component D, except that the blue flavodoxin semiquinone eluted from the DEAE-Sepharose column at 0.4 M NaCl in a volume of 60 mL. The flavodoxin-containing fractions were pooled and concentrated by ultrafiltration (YM 3 filter, Amicon) to a volume

of 2 mL. The protein was applied to a Superose 12 column (2 × 60 cm), which was equilibrated with 5 volumes of buffer B (20 mM Mops, pH 7.2, 0.3 M NaCl, 2 mM dithiothreitol). Elution of the flavodoxin occurred at a buffer volume which corresponded to a molecular mass of ca. 13 kDa. The fractions were diluted to 50 mM NaCl. To remove final impurities, chromatography on a Q-Sepharose high-performance column (1.6 × 14 cm) was performed. The column was equilibrated with 5 volumes of buffer A, and the homogeneous flavodoxin was eluted with a linear NaCl gradient (0−0.7 M NaCl in 400 mL of buffer A). The protein could be stored anoxically at −80 °C. To determine the difference in the extinction coefficients of the hydroquinone/semiquinone transition of flavodoxin, the blue form of the protein was reduced with sodium dithionite. After removal of excess reductant, the difference spectrum yielded $\Delta\epsilon_{578} = +4.0\ mM^{-1}\ cm^{-1}$.

Electron Transfer from Component A to Component D. Component A was reduced by incubating the enzyme with a 10−100-fold excess of sodium dithionite in 50 mM Tris/HCl, pH 8.0, 0.3 M NaCl, 10 mM $MgCl_2$, 0.1 mM ADP for 10 min at 20 °C, followed by gel filtration on Sephadex G25 using the same buffer to remove the reducing agent. UV−visible spectroscopy was performed to prove a complete separation of dithionite. Component D was used as isolated in 20 mM Mops, pH 7.2, 1 mM dithiothreitol. Equimolar mixtures of reduced component A and component D (both at 0.2−0.4 mM final protein concentration) were prepared. ADP, or ATP, or ATP and the substrate (*R*)-2-hydroxyglutaryl-CoA were added. At different incubation times at 20 °C, the solutions were anoxically frozen using liquid nitrogen. Changes of the redox states of the proteins were monitored by EPR and Mössbauer spectroscopy. For Mössbauer spectroscopy, only one protein component was labeled with ^{57}Fe in order to distinguish between the Fe−S clusters of components A and D. The reactions were complete after less than 2 min, since samples taken after 2, 5, and 20 min incubation time exhibited equal spectral properties.

Electron Transfer from Flavodoxin Hydroquinone to Component A. Flavodoxin was reduced in 50 mM Tris/HCl, pH 8.0, using a 10-fold excess of dithionite, analogous to the reduction of component A. The oxidation of component A was performed in 50 mM Tris/HCl, pH 8.0, 0.3 M NaCl, 10 mM $MgCl_2$, and 0.1 mM ADP by using a 10-fold excess of thionine. The oxidizing agent was removed by gel filtration with Sephadex-G25. UV−visible spectra were recorded with single proteins (6−10 μM each) and with equimolar mixtures.

RESULTS

Isolation of a 16 kDa Flavodoxin. When *A. fermentans* was grown on glutamate under iron limiting conditions (1−2 μM Fe in the medium), the soluble cell fraction contained a blue−violet air-oxidizable protein fraction, which eluted from the DEAE-Sepharose column at higher ionic strength (0.4 M NaCl) than component D of 2-hydroxyglutaryl-CoA dehydratase (0.2 M NaCl, see Materials and Methods). Further purification of the blue protein by gel filtration on Superose 12 followed by anion exchange chromatography on Q-Sepharose resulted in a preparation consisting of a single polypeptide of 16 kDa as revealed by SDS-PAGE

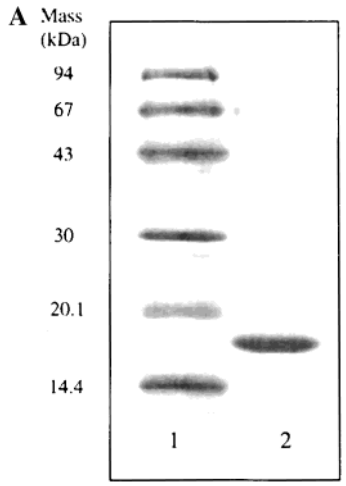

B

A. fermentans[1]	MSKIAVXFWSGTGNTEAMAKAVEEGAKGKGA	100
T. denticola[2]	MAKIAVIYWSGTGNTQSMAESVLEGLKAGGA	67
C. pasteurianum[3]	-MKVNIIYWSGTGNTEAMAKLIAEGAQEKGA	66
C. acetobutylicum[4]	MVKINIIYCSGTGNTEAMANLISEGAKSAGA	59
M. elsdenii[5]	--MVEIVYWSGTGNTEAMANEIEAAVKAAGA	54
C. difficile 1[6]	-----MLYQTRSGNTERVAKLIEEGAKKVDG	40
C. beijerinckii[7]	---MKIVYWSGTGNTEKMAELIAKGIIESGK	37
D. vulgaris[8]	MPKALIVYGSTTGNTEYTAETIARELADAGY	33
C. difficile 2[6]	-MKSLVLYSSLTGNTKKIAYTIYDEIQEEKD	24

FIGURE 1: Molecular properties of the flavodoxin from *A. fermentans*. (A) SDS−PAGE prepared from 15% acrylamide. The gel was loaded with molecular mass markers (lane 1) and 5 mg of flavodoxin. (B) Sequence of the N-terminus and comparison with those of flavodoxins from various organisms. *T.*, *Treponema*; *C.*, *Clostridium*; *M.*, *Megasphaera*; *D.*, *Desulfovibrio*. The numbers at the end of each line indicate the sequence identities with the N-terminus of the flavodoxin from *A. fermentans*: 1, this paper; 2, from unfinished genome data at TIGR, http://www.tigr.org/; 3, (*37*); 4, from unfinished genome data by the DOE Joint Genome Institute; 5, (*38*, *39*); 6, from unfinished genome data at http://www.sanger.ac.uk/Projects/C_difficile/blast_server.shtml; 7, (*40*); 8, (*41*).

(Figure 1A). N-Terminal sequencing by Edman degradation yielded an amino acid sequence (30 residues) with high identities to those of isolated flavodoxins and deduced flavodoxins from anaerobic organisms (Figure 1B). Upon heating of the flavodoxin (1 mg mL^{-1}, pH 7.0) to 75 °C for 20 min under air, the protein precipitated and released 1.0 ± 0.1 FMN per monomer into the supernatant as identified by HPLC (*23*) and quantified by the absorbancies at λ = 450 nm ($\epsilon = 11.3\ mM^{-1}\ cm^{-1}$) and at λ = 370 nm ($\epsilon = 10.7\ mM^{-1}\ cm^{-1}$) (*24*). The blue−violet color of the anoxically isolated protein suggested the neutral semiquinone state of the FMN, which was confirmed by the UV−visible spectrum. It showed the typical absorption of neutral semiquinone flavin radicals between λ = 400 and 670 nm with a maximum at 578 nm (Figure 2) (*25*). Furthermore, a quasi-isotropic EPR spectrum could be measured from frozen solutions, which revealed 1.0 ± 0.2 spin/mol as expected. The apparent line width was 2 mT, which decreased to 1.5 mT when the protein was dissolved in D_2O (Figure 3). Both the width of the EPR signal and its solvent dependence are well-known for neutral, protonated flavin semiquinone radicals, in which coupling of the electron spin with that of the proton broadens the signal. In unprotonated anionic flavin semiquinones, no such solvent dependence of the EPR signal width can be observed (*26*). Redox titration of the flavodoxin revealed a midpoint potential of −60 mV for the semi-

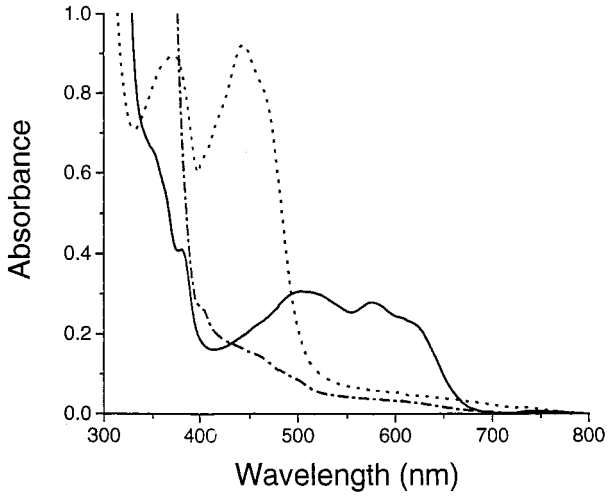

FIGURE 2: UV−visible spectra of the three redox states of the flavodoxin from *A. fermentans*. The different redox states of the flavodoxin were prepared as described under Materials and Methods. Dotted line, oxidized, benzoquinone state; solid line, neutral blue semiquinone state; dashed line, reduced, hydroquinone state. The protein concentration in all samples was 70 μM.

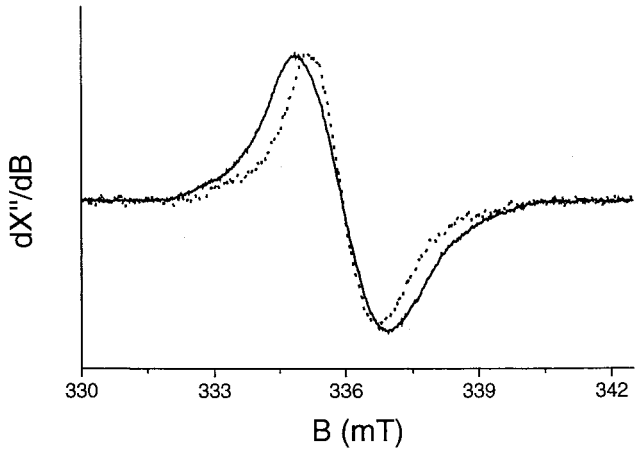

FIGURE 3: EPR spectrum of the neutral flavodoxin semiquinone from *A. fermentans*. Solid line, flavodoxin semiquinone in H_2O, protein concentration 50 μM, spin concentration 50 ± 10 μM; dotted line, flavodoxin semiquinone in D_2O, protein concentration 10 μM, spin concentration 7 ± 2 μM. EPR settings: frequency 9.434 GHz, temperature 80 K, modulation amplitude 0.5 mT, microwave power 20 mW.

quinone/benzoquinone couple and −430 mV for the hydroquinone/semiquinone couple at pH 7.0.

The hydroquinone form of the flavodoxin could replace the reducing agent titanium(III) citrate in the activity assay of 2-hydroxyglutaryl-CoA dehydratase, suggesting that this protein may act as the natural electron donor for component A of this enzyme. Neither the benzoquinone state nor the semiquinone state of the flavodoxin was capable of activating the enzyme. Whereas the activation with titanium(III) citrate required a 100-fold molar excess over component A (*8*), only a 6-fold excess of flavodoxin hydroquinone was necessary to yield full activity. UV−visible studies confirmed a spontaneous electron transfer from reduced flavodoxin hydroquinone to component A. To further corroborate the occurrence of this transfer, component A was oxidized to the $[4Fe\text{-}4S]^{2+}$ form with a 10-fold excess of thionine for 10 min followed by separation from low molecular mass compounds by gel filtration on Sephadex G-25. The resulting

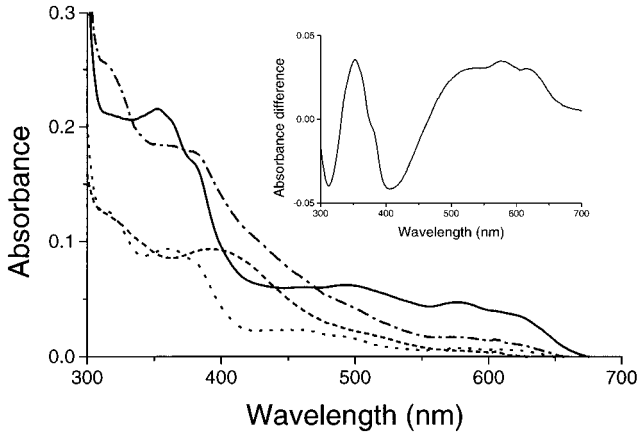

FIGURE 4: UV−visible spectroscopic studies on the electron transfer between flavodoxin hydroquinone and oxidized component A. Flavodoxin was dissolved in 50 mM Tris/HCl, pH 8.0; component A was dissolved in 50 mM Tris/HCl, pH 8.0, 0.3 M NaCl, 10 mM $MgCl_2$, and 1 mM ADP. The dotted line shows the spectrum of 6 μM flavodoxin hydroquinone; the dashed line shows the spectrum of 6 μM oxidized component A. The dash−dotted line is a theoretical sum spectrum of both single proteins. The solid line exhibits the recorded spectrum of an equimolar mixture of both proteins, 6 μM each. The inset shows the difference spectrum of the solid line minus oxidized component A + flavodoxin hydroquinone (dash−dotted in the main figure). The absorbance between 460 and 700 nm is due to the flavodoxin semiquinone (cf. Figure 2).

spectrum of equimolar mixtures of flavodoxin hydroquinone and oxidized $[4Fe\text{-}4S]^{2+}$ cluster containing component A differed significantly from the sum of the spectra of both protein components before mixing (Figure 4). At λ = 450−670 nm, the typical absorption pattern of the neutral flavodoxin semiquinone radical showed up, while the absorption around λ = 420 nm decreased due to reduction of the $[4Fe\text{-}4S]^{2+}$ cluster of component A. Using the measured extinction coefficient at 578 nm for the hydroquinone/semiquinone transition, $\Delta\epsilon = +4.0$ mM^{-1} cm^{-1}, and that at 400 nm for the reduction of the $[4Fe\text{-}4S]^{2+}$ cluster, $\Delta\epsilon = -4.5$ mM^{-1} cm^{-1} (see Materials and Methods), it was calculated that the electrons were almost quantitatively transferred from the hydroquinone to the $[4Fe\text{-}4S]^{2+}$ cluster of component A. Control experiments indicated that flavodoxin hydroquinone was not able to reduce the $[4Fe\text{-}4S]^{2+}$ cluster of component D. Furthermore, omission of component A in the assay of 2-hydroxyglutaryl-CoA dehydratase with flavodoxin hydroquinone as reducing agent gave no activity.

Interaction of Component A with ATP. Previous experiments suggested a destruction of the $[4Fe\text{-}4S]^{2+}$ cluster of component A by incubation with the iron chelator bathophenanthroline disulfonate (*7*). The experiments were repeated under strict anaerobic conditions, whereby the rate of the formation of the iron chelate was determined spectrophotometrically at λ = 535 nm (ϵ = 22 mM^{-1} cm^{-1}). The cuvette contained 35 mM Tris/HCl, pH 8.0, 5 mM bathophenanthroline disulfonate, and either 1.0 mM ADP or 1.0 mM ATP. The reaction was initiated by addition of 20 μM reduced or oxidized component A and 1 mM $MgCl_2$ (final concentrations). In the presence of ADP, the initial chelation rate was 3 μM min^{-1}, whereas ATP enhanced the initial rate to 24 μM min^{-1}, regardless of whether component A was in the oxidized or in the reduced form. In the presence of ATP, the reaction was completed within 5 min and showed

that all four iron atoms were removed from the protein. There was no difference whether component A was in the reduced or in the oxidized form.

In an earlier paper, a weak ATPase activity of component A was described (*2*). Since in that work the oxidation state of component A was not defined, we repeated the experiment with completely oxidized component A. The ATPase activity was measured in a coupled NADH-dependent assay with phosphoenolpyruvate in the presence of 10 mM $MgCl_2$ and gave values between 6 and 4 s^{-1} depending on the preparation. The K_m value for ATP was estimated as 3 μM. In the reduced state, component A showed very low ATPase activity (<0.1 s^{-1}), which could have even been due to traces of oxidized component A. In a typical experiment, the addition of 1 μM component D to an assay with 1 μM reduced component A caused an increase in the ATPase activity from <0.1 to 3.0 s^{-1}; subsequent addition of 1 mM (*R*)-2-hydroxyglutaryl-CoA yielded a slight further increase to 3.2 s^{-1}.

Electron Transfer from Component A to D followed by EPR and Mössbauer Spectroscopy. Equimolar mixtures of *oxidized* component D (as isolated) and *reduced* component A were prepared with 5 mM $MgCl_2$ and either 10 mM ADP, or 10 mM ATP, or 10 mM ATP + 1 mM (*R*)-2-hydroxyglutaryl-CoA, or 10 mM AMP-PNP, to examine a possible effect of these molecules on the electron transfer. UV−visible spectra indicated that the FMN of component D remained in the reduced state under all conditions employed. The redox behavior of the different iron−sulfur centers in the enzyme components, which hardly can be disentangled from the electronic absorption spectra, was investigated by using EPR and Mössbauer spectroscopy (Figures 5−9). Components A and D are discernible from their EPR spectra due to different *g* values: Reduced component A shows a rather unusual $S = 3/2$ spectrum ($g = 4-6$), whereas for component D only a $[3Fe\text{-}4S]^+$ signal from oxidatively degraded cubane clusters in the oxidized state is known (*7*). Assignments of the Mössbauer spectra could be achieved by selective labeling with ^{57}Fe [component A(57-Fe) and component D(57-Fe), respectively]. At 80 K, oxidized and reduced Fe−S clusters are expected to show pure quadrupole doublets with distinct Mössbauer parameters, due to either $S = 0$ ground state or fast spin relaxation. The difference of the respective subspectra is even more pronounced at 4.2 K, because the oxidized cubanes again yield virtually unsplit doublets ($S = 0$ ground state), whereas the reduced centers show wide magnetic hyperfine splittings due to slow spin relaxation and $S = 1/2$ or 3/2 ground states.

In the presence of ADP, the mixture of both proteins did not show significant electron transfer from component A to component D. The $S = 3/2$ EPR signals of the $[4Fe\text{-}4S]^+$ cluster of reduced component A are clearly detectable, and new signals did not appear (Figures 5A and 8A). The EPR spectrum was simulated according to our previous EPR investigations by using a distribution of rhombicities, *E*/*D*, and *g* values, which is supposed to represent geometrical strain of the $[4Fe\text{-}4S]^+$ cluster (*7*). The 80 K Mössbauer spectrum of the component A(57-Fe) preparation consists of a slightly asymmetric quadrupole doublet, which could be simulated by two subspectra due to the presence of 19% oxidized $[4Fe\text{-}4S]^{2+}$ cluster and 81% reduced $[4Fe\text{-}4S]^{1+}$ cluster (Figure 6A). The composition of the subspectra was

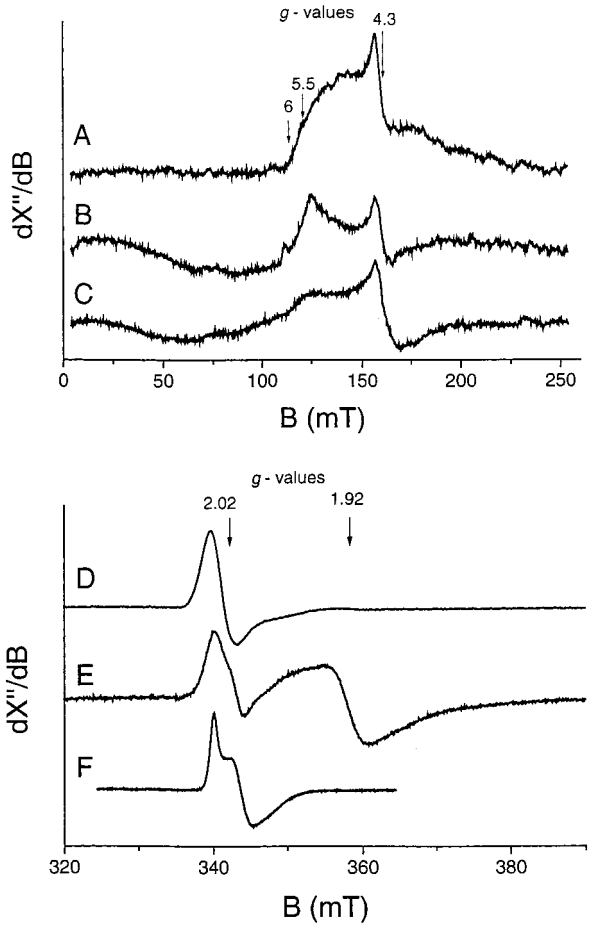

FIGURE 5: ATP-dependent electron transfer from reduced component A to component D as analyzed by EPR spectroscopy. The EPR tubes contained 150 μM reduced component A, 150 μM component D in 50 mM Tris/HCl, pH 8.0, 150 mM NaCl, 5 mM $MgCl_2$, 0.5 mM ADP, and 10 mM Mops, pH 7.0. In addition, the tubes contained 10 mM ADP (tubes A and D), 10 mM ATP (B and E), or 10 mM ATP and 1 mM 2-hydroxyglutaryl-CoA (C and F). Conditions of the EPR experiments: frequency 9.634 GHz, temperature 10 K, modulation amplitude 12.8 G, microwave power 20 mW in spectra A−C and 0.1 mW in spectra D−F.

corroborated by the magnetic spectrum recorded at 4.2 K (Figure 6A′). In contrast, the $[4Fe\text{-}4S]^{2+}$ cluster of component D(57-Fe) is found from its Mössbauer parameters to be fully oxidized (Figure 7A). At 4.2 K with weak applied field, a quadrupole spectrum without resolved magnetic splittings is observed due to the $S = 0$ ground state of the oxidized cubane clusters. Particularly the isomer shift (δ) would increase from 0.44 to 0.53 mm s^{-1} upon a possible reduction of the cluster. The EPR spectrum is in accordance with this interpretation, since it shows only trace amounts (<10%) of a $[3Fe\text{-}4S]^+$ signal at $g = 2.02$ (Figure 5D), which most probably represents an inactive enzyme species. In the 4.2 K Mössbauer spectrum, the very broad paramagnetic spectrum of the $[3Fe\text{-}4S]^+$ cluster is virtually not detected (Figure 7A).

In the presence of ATP, the $[4Fe\text{-}4S]^{1+}$ cluster of component A(57-Fe) became oxidized from 19% to 38% as judged by Mössbauer spectroscopy (Figure 6B,B′). The $[4Fe\text{-}4S]^{2+}$ cluster of component D(57-Fe), however, remained unaffected (Figure 7B). We note that the *g* values of the $S = 3/2$ $[4Fe\text{-}4S]^+$ cluster of the remaining reduced component A changed significantly with incubation of ATP (Figure 5B).

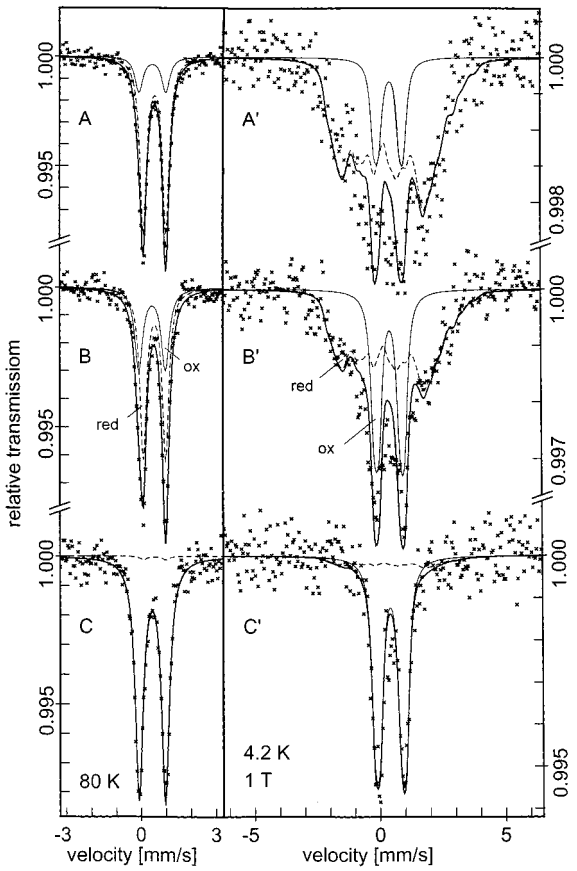

FIGURE 6: ATP-dependent electron transfer from reduced ^{57}Fe-labeled component A to component D as analyzed by Mössbauer spectroscopy at 80 and 4.2 K. The samples were prepared as described in Figure 5; the concentrations of components A (57-Fe) and D were 400 μM each. Spectra A, A′, addition of 10 mM ADP; B, B′, addition of 10 mM ATP; C, C′, addition of 10 mM ATP and 1 mM (*R*)-2-hydroxyglutaryl-CoA. Spectra A−C were recorded at 80 K without applied field. The boldface solid lines are simultaneous simulations (see Materials and Methods) using two quadrupole doublets. Subspectrum "ox" (thin solid line, $\delta = 0.44$ mm/s, $\Delta E_Q = 1.06$ mm/s, $\Gamma = 0.38$ mm/s), oxidized [4Fe-4S]$^{2+}$ cluster; subspectrum "red" (dashed line, $\delta = 0.53$ mm/s, $\Delta E_Q = 0.90$ mm/s, $\Gamma = 0.32$ mm/s), reduced [4Fe-4S]$^{+}$ cluster with relative abundances of the "ox" subspectrum of 19% in (A), 38% in (B), and 98% in (C). Spectra A′−C′ were measured at 4.2 K with 1 T applied perpendicular to the gamma rays. The thin solid line ("ox") is a magnetic simulation with $S = 0$ and the parameters of the corresponding 80 K component (ΔE_Q positive, asymmetry parameter $\eta = 0$). The dotted line "red" is a spin Hamiltonian simulation for $S = 3/2$ with parameters taken from (*7*) and relative intensities taken from the zero-field spectra.

A new signal appeared at $g = 5.5$, indicating large rhombicity $E/D \approx 0.33$, which was never observed when reduced component A was investigated separately in the absence of component D but in the presence of ATP. Since it seems to be established that $S = 3/2$ EPR signals of [4Fe-4S]$^{+}$ clusters are very sensitive to changes of surrounding protein conformations (*7*, *27*−*29*), we assign the spectral changes to ATP-induced protein interactions between components A and D. Surprisingly, a distinct new EPR signal at g values <2 appeared in the ATP-containing enzyme preparations (Figure 5E). Due to the unusual properties, which are not consistent with those of high-spin or low-spin iron centers, it is very unlikely that this spectrum originates from a [4Fe-4S]$^{+}$ cluster as will be discussed below.

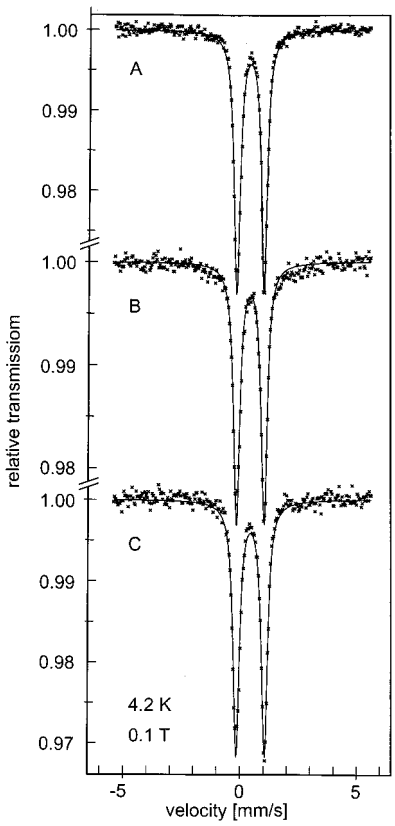

FIGURE 7: ATP-dependent electron transfer from reduced component A to ^{57}Fe-labeled component D as analyzed by Mössbauer spectroscopy at 4.2 K. The samples were prepared as described in Figure 5; the concentrations of components A and D (57-Fe) were 300 μM each. All spectra were taken with an external magnetic field of 0.1 T. Spectrum A, addition of 10 mM ADP; B, addition of 10 mM ATP; C, addition of 10 mM ATP and 1 mM (*R*)-2-hydroxyglutaryl-CoA. All three spectra could be simulated by using the following parameters: $\delta = 0.44$ mm/s, $\Delta E_Q = 1.20$ mm/s, $\eta = 0.7$, $\Gamma = 0.32$ mm/s, $S = 0$. These parameters are characteristic for $Fe^{2.5+}$ in a tetrahedral sulfur coordination as observed in a [4Fe-4S]$^{2+}$ cluster.

The presence of the substrate (*R*)-2-hydroxyglutaryl-CoA in addition to ATP increased the amount of oxidized [4Fe-4S]$^{+}$ cluster of component A from 38% to more than 90% as indicated by Mössbauer spectroscopy (Figure 6C,C′), whereas the [4Fe-4S]$^{2+}$ cluster of component D again did not change its redox state (Figure 7C). EPR spectroscopy revealed that the remaining <10% of reduced component A occurred in the same state as in the presence of ADP (Figure 5C). Hence, the interaction of that fraction with component D has disappeared. Furthermore, also the new EPR signal at $g < 2$ has vanished (Figure 5F).

Since similar EPR spectra were obtained by replacing ATP by the nonhydrolyzable analogue AMP-PNP, hydrolysis of ATP seems not be necessary to promote these effects (Figure 8). However, we were not able to quantify the amount of oxidized component A after AMP-PNP treatment. Mössbauer experiments could not be performed because component A could not be concentrated in the presence of AMP-PNP to >0.1 mM.

The new EPR signal, which appeared in the presence of ATP, but also of AMP-PNP (Figures 5E, 8D,E), could be readily simulated with g values of 1.97, 1.92, and 1.88 as depicted in Figure 9. The overall appearance of the spectrum, its temperature dependence, and particularly the low average

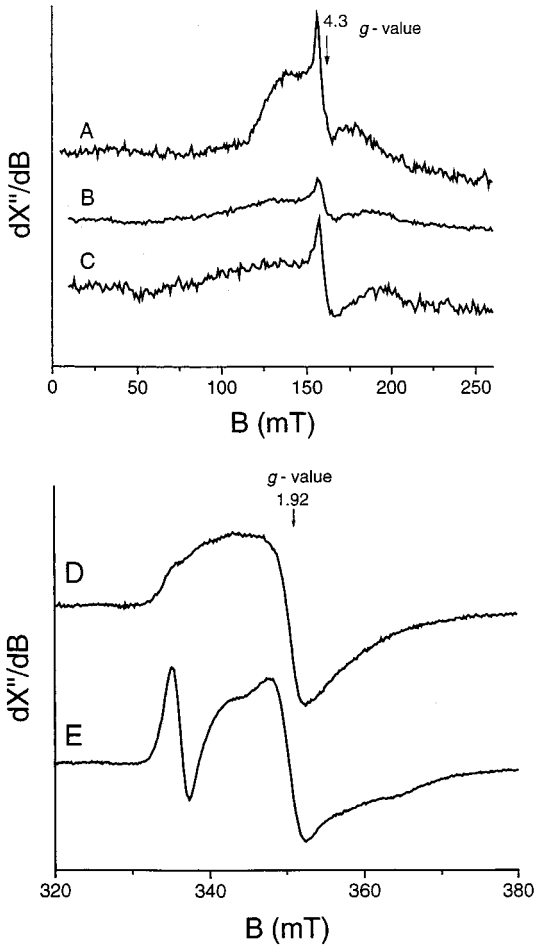

FIGURE 8: AMP-PNP-dependent electron transfer from reduced component A to component D as analyzed by EPR spectroscopy. The EPR tubes contained 150 μM reduced component A, 150 μM component D in 50 mM Tris/HCl, pH 8.0, 150 mM NaCl, 5 mM $MgCl_2$, 0.5 mM ADP, and 10 mM Mops, pH 7.0. Tube A contained in addition 10 mM ADP, tubes B and E 10 mM AMP-PNP, tube C 10 mM AMP-PNP and 1 mM (*R*)-2-hydroxyglutaryl-CoA, and tube D 10 mM ATP. Conditions of the EPR experiments: frequency 9.634 GHz, temperature 10 K, modulation amplitude 12.8 G, microwave power 20 mW in spectra A−C and 0.1 mW in spectra D and E.

g value are not consistent with an interpretation of a reduced $S = 1/2$ $[4Fe\text{-}4S]^+$ cluster, or any other known high-spin or low-spin iron center. Typical spectra of such species always exhibit one component of the *g* matrix to be >2, for iron−sulfur clusters usually in the range $g = 2.04-2.06$ (*30*). Furthermore, any contribution of a paramagnetic $[4Fe\text{-}4S]^+$ cluster to the Mössbauer spectrum of component D (Figure 7B) would have resulted in a hyperfine structure, which cannot be seen. The *g* values of the new EPR signal closely resemble those of d^1-metal species such as Mo(V) or W(V) (*31*−*33*). However, these d^1-metal EPR signals usually can be observed at temperatures up to 100 K, whereas the signal described here already disappeared at temperatures of about 50−60 K due to excessive line broadening by fast spin relaxation. Nevertheless, we assume that the new signal might well represent a d^1-metal ion. The intrinsic spin relaxation rates can be increased in a protein moiety by weak spin−spin interaction with the excited paramagnetic $S = 1$, 2, ... spin states of the oxidized $[4Fe\text{-}4S]^{2+}$ cluster in component D. Moura and co-workers described very similar observations for the tungsten-dependent formate dehydrogenase, where a [4Fe-4S] cluster enhanced the relaxation of the W(V) center (*34*).[2] In fact, metal analyses of highly pure component D preparations (>95% as judged by SDS−PAGE) using neutron activation and atomic absorption spectroscopy (AAS) revealed 0.07−0.2 molybdenum/heterodimer. The low values are in accordance with quantifications of the corresponding EPR signal, which amounted on average up to 0.2 spin/heterodimer depending on the preparation. Furthermore, biochemical enzyme activity experiments also indicated a physiological role of this metal because component D activity and molybdenum concentration eluted together in the same peak from the UnoQ6-Sepharose column (Figure 10). Unfortunately, growth experiments with *A. fermentans* failed to proof an essential requirement of molybdenum for the organism. The large amount of yeast extract present in the medium (0.5%) prevented sufficient sensitivity. Finally, addition of 1−10 mM molybdate to the medium or up to 100 mM molybdate to the assay gave no increase of the Mo content of the enzyme or increase in enzymatic activity, respectively. Hence, the putative role of molybdenum and its function in 2-hydroxyglutaryl-CoA dehydratase need further investigation.

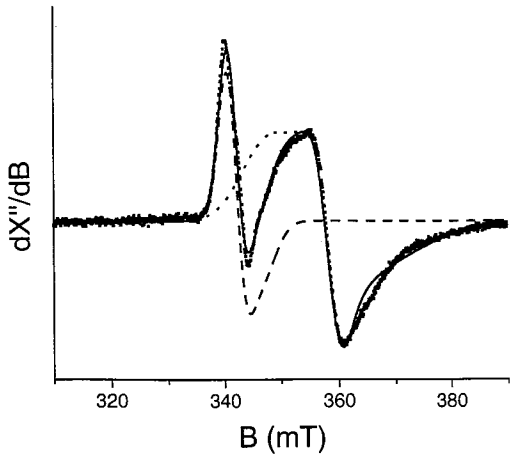

FIGURE 9: Simulation of the EPR spectrum assigned to reduced component D (Figure 5E). The signal around 340 mT was simulated with parameters for an $S = 1/2$ $[4Fe\text{-}4S]^+$ cluster with $g = 2.015$, 2.015, 1.983 and (Gaussian) line widths = 4.6, 4.6, 6.7 mT (dashed line). The signal around 350−360 mT was simulated with parameters for d^1-metals such as Mo(V) or W(V) with $g = 1.97$, 1.92, 1.86 and line widths = 14.4, 4.5, 26.8 (dotted line). The parameters are untypical for $S = 1/2$ $[4Fe\text{-}4S]^+$ clusters, because in the spectra of these species one *g* component exhibits a value >2 (2.03−2.08). However, the data of the latter spectrum are similar to the spectra observed for d^1-metals such as Mo(V) or W(V). The solid line shows the simulation of the overall spectrum composed of the two independent EPR signals. It fits well to the observed spectrum.

DISCUSSION

The results of this work are interpreted as evidence for an ATP-driven electron transfer from flavodoxin via component

[2] Unfortunately, such processes cannot be followed by Mössbauer spectroscopy because the paramagentic excited states of the $[4Fe\text{-}4S]^{2+}$ cluster are significantly populated only at temperatures above 50−100 K. In this regime, however, the spin relaxation is already in the fast limit with respect to the ^{57}Fe nuclear precession rates. Since, furthermore, the population differences of the electronic spin levels are small (spin-up vs spin-down), the effective hyperfine fields are vanishing small and, hence, the effects of very weak inter-center spin couplings ($|J| \ll 1$ cm^{-1}) are far beyond the detection limits.

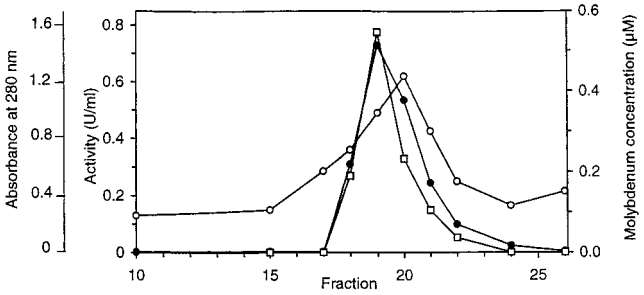

FIGURE 10: Coelution of component D activity and molybdenum. Partially purified component D of 2-hydroxyglutaryl-CoA dehydratase in 20 mM Mops, pH 7.0, was eluted at 250 mM NaCl from a UnoQ6-Sepharose high-performance column (Pharmacia) by applying a linear NaCl gradient. The fractions were assayed for protein (absorbance at 280 nm, open circles), dehydratase activity (closed circles), and concentration of molybdenum (open squares).

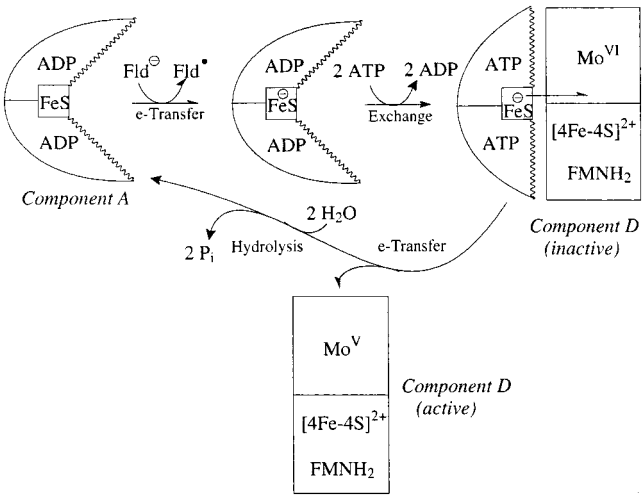

FIGURE 11: Model of the electron transfer from flavodoxin via component A to component D. The wavy lines in component A should indicate the two cluster helices; Fld, flavodoxin; FeS, [4Fe-4S]$^{2+}$ cluster; FeS^{-}, [4Fe-4S]$^{+}$ cluster. Mo(V) is supposed to supply the electron required in Scheme 1.

A and component D to the thiol ester carbonyl as outlined in Figure 11. In the equimolar mixture of flavodoxin hydroquinone with oxidized component A, one electron is almost quantitatively transferred; the [4Fe-4S] cluster of component A becomes fully reduced, and the flavodoxin semioquinone is formed. Hence, the redox potential of component A must be at least 100 mV more positive than that of the flavodoxin hydroquinone/semiquinone couple, which was determined as −430 mV. A direct determination of the redox potential of component A was not possible, since the protein precipitated upon addition of organic dyes. Furthermore, the redox state of component A could only be measured by Mössbauer spectroscopy, which required large amounts of protein. Quantification by EPR spectroscopy could not be achieved with sufficient accuracy due to the intrinsically broad powder spectra of the spin 3/2 system.

Component A is distinguished from many other [4Fe-4S] cluster containing proteins by its extreme oxygen sensitivity and its accessibility to iron chelating agents. The structure of component A in the presence of ADP reveals that the [4Fe-4S] cluster is exposed to the solvent and thus explains these properties (*9*). Exchange of the bound ADP by ATP enhances the iron chelation rate by bathophenanthrolinedisulfonate 8-fold, which suggests a large conformational change induced by ATP. A similar but somewhat different situation has been found in the iron protein of nitrogenase from *Azotobacter vinelandii*. In the absence of a nucleotide, the iron protein is stable in the presence of the iron chelator α,α′-bipyridyl (2 mM), whereas addition of 5 mM ATP-Mg^{2+} initiates a significant chelation rate. Removal of half of the ATP by 2.5 mM glucose and hexokinase immediately stops the chelation, which indicates an inhibition by the tighter binding ADP (*10*). Since no structural data for the component A−ATP complex are available yet, one has to be guided by data obtained for the nitrogenase iron protein. Its [4Fe-4S] cluster also is located between two 'cluster helices'. The angle helix−[4Fe-4S]−helix is 150°, 45° larger than in component A. Upon formation of the complex of the iron protein with the MoFe protein in the presence of ADP−AlF_4^-, a transition-state analogue of ATP hydrolysis, the angle enlarges from 150° to 180°, whereby the [4Fe-4S] cluster would become much more exposed to the solvent unless bound to the MoFe protein. This 'opening' of the angle moves the [4Fe-4S] cluster by about 4 Å toward the MoFe protein and thus facilitates the electron transfer to the P-cluster (*35*). In the case of component A, the angle could possibly enlarge upon ATP binding by 75° up to 180°, which could move the cluster 13 Å toward component D. Hence, component A is probably able to switch between the open (180°) and the closed (105°) conformation, which is driven by ATP hydrolysis as shown in Figure 11.

In the oxidized [4Fe-4S]$^{2+}$ state, component A exhibits high ATPase activity of 4−6 s^{-1}. The low apparent $K_m = 3$ μM for ATP indicates saturation under all normal physiological conditions. Upon reduction of component A by one electron, however, the ATPase activity is abolished. Therefore, the open conformation is retained in the reduced state. Probably in vivo component A is always 'loaded' with one electron and two molecules of ATP until it encounters component D, whereby the electron is transferred and hydrolysis resumes. The exchange of ADP bound to reduced component A by ATP probably lowers the reduction potential of the [4Fe-4S]$^{1+/2+}$ cluster by at least 100 mV as observed with the nitrogenase iron protein (*36*).

Although the oxidation of component A can be clearly shown by Mössbauer spectroscopy, the resulting reduction of component D cannot so readily be seen, since the expected change in the oxidation states of the [4Fe-4S]$^{2+}$ cluster and the $FMNH_2$ of component D did not occur. The only observable change is the formation of the d^1 EPR signal attributed to Mo(V), which, however, does not account for more than 20% of the amount of component D present in the incubation. On the other hand, this agrees well with the increase of the amount oxidized component A from 19% to only 38% after electron transfer to component D as shown in Figure 6B,B′. Upon subsequent addition of the substrate, the putative Mo(V) signal disappears, which may due to the further electron transfer to the substrate. The formation of the Mo(V) signal can also be detected by replacing ATP by its nonhydrolyzable analogue AMP-PNP. This correlates with the proposed reaction scheme as shown in Figure 11. Hydrolysis of ATP, by which component A returns to the oxidized closed conformation, is only necessary *after* the electron has been transferred to component D, which hands it further to the substrate. Thus, the next reduction of component A and all subsequent catalytic turnovers are

blocked, consistent with the inhibitory action of AMP-PNP (*6*). Under the condition of the experiment with a 1:1 ratio of component A/component D, only a single turnover occurred. Hence, no inhibition by the ATP analogue could be observed.

It should be noted that the EPR spectra show neither the postulated ketyl radical anions nor the enoxy radical (Scheme 1). The possibility that the organic radicals are concealed to EPR spectroscopy by interaction with the $[4Fe\text{-}4S]^{2+}$ cluster can be dismissed, since this interaction would have been detected by Mössbauer spectroscopy. A speculative explanation could be a second, probably much slower electron transfer from component D to the substrate. Thereby the enoxy radical would be reduced to the enolate followed by protonation to yield glutaryl-CoA. This additional electron transfer could also account for the complete oxidation of component A in the presence of ATP and substrate. Although glutaryl-CoA has never been detected under steady-state conditions, it might be possible that under equilibrium conditions, as employed in the experiments of Figures 6 and 7, this CoA derivative is formed at a concentration of up to 50% of that of reduced component A.

Finally, the mode of electron transfer proposed in Figure 11 is apparently not consistent with the EPR spectrum of Figure 5B, whose signal at $g = 5.5$ has been interpreted as an interaction of component A with component D. In Figure 11, the interaction of reduced component A loaded with ATP with component D is followed by an immediate electron transfer to Mo(VI) with subsequent release of oxidized component A and hydrolysis of ATP. Hence, this interaction should have been *transient* rather than *persistent* as observed under the employed conditions (incubation for ≥2 min at 20 °C). The persistent interaction could be due to the fact that ≥80% of component D contains no molybdenum and therefore no acceptor for electron transfer. Thus, component A together with ATP and molybdenum-free component D may form an unproductive but probably tight complex.

ACKNOWLEDGMENT

We thank Mrs. Iris Schall (Philipps-Universität) for excellent technical assistance.

REFERENCES

1. Buckel, W. (1980) *Eur. J. Biochem. 106*, 439−447.
2. Müller, U., and Buckel, W. (1995) *Eur. J. Biochem. 230*, 698−704.
3. Buckel, W., and Barker, H. A. (1974) *J. Bacteriol. 117*, 1248−1260.
4. Härtel, U., and Buckel, W. (1996) *Arch. Microbiol. 166*, 350−356.
5. Buckel, W. (2001) *Appl. Microbiol. Biotechnol. 57*, 263−273.
6. Schweiger, G., Dutscho, R., and Buckel, W. (1987) *Eur. J. Biochem. 169*, 441−448.
7. Hans, M., Buckel, W., and Bill, E. (2000) *Eur. J. Biochem. 267*, 7082−7093.
8. Klees, A. G., Linder, D., and Buckel, W. (1992) *Arch. Microbiol. 158*, 294−301.
9. Locher, K. P., Hans, M., Yeh, A. P., Schmid, B., Buckel, W., and Rees, D. C. (2001) *J. Mol. Biol. 307*, 297−308.
10. Howard, J. B., and Rees, D. C. (1996) *Chem. Rev. 96*, 2965−2982.
11. Buckel, W., and Keese, R. (1995) *Angew. Chem., Int. Ed. Engl. 34*, 1502−1506.
12. Buckel, W. (1996) *FEBS Lett. 389*, 20−24.
13. Mack, M., Bendrat, K., Zelder, O., Eckel, E., Linder, D., and Buckel, W. (1994) *Eur. J. Biochem. 226*, 41−51.
14. Buckel, W., Ziegert, K., and Eggerer, H. (1973) *Eur. J. Biochem. 37*, 295−304.
15. Riddles, P. W., Blakeley, R. L., and Zerner, B. (1979) *Anal. Biochem. 94*, 75−81.
16. Buckel, W. (1986) *Methods Enzymol. 125*, 547−558.
17. Bradford, M. M. (1976) *Anal. Biochem. 72*, 248−254.
18. Smith, P. K., Krohn, R. I., Hermanson, G. T., Mallia, A. K., Gartner, F. H., Provenzano, M. D., Fuyimoto, E. K., Goeke, N. M., Olson, B. J., and Klenk, D. C. (1985) *Anal. Biochem. 150*, 76−85.
19. Hans, M., Sievers, J., Müller, U., Bill, E., Vorholt, J. A., Linder, D., and Buckel, W. (1999) *Eur. J. Biochem. 265*, 404−414.
20. Fish, W. W. (1988) *Methods Enzymol. 158*, 661−668.
21. Cline, J. D. (1969) *Limnol. Oceanogr. 14*, 454−458.
22. Hans, M., and Buckel, W. (2000) *BIO TECH Int. 12*, 12.
23. Eikmanns, U., and Buckel, W. (1991) *Eur. J. Biochem. 197*, 661−668.
24. Dawson, R. M. C., Elliot, D. C. E., Elliot, W. H., and Jones, K. M. (1989) *Data for Biochemical Research*, Oxford Science Publications, Oxford.
25. Biel, S., Klimmek, O., Gross, R., and Kröger, A. (1996) *Arch. Microbiol. 166*, 122−127.
26. Çinkaya, I., Buckel, W., Medina, M., Gomez-Moreno, C., and Cammack, R. (1997) *Biol. Chem. Hoppe-Seyler 378*, 843−849.
27. Lindahl, P. A., Day, E. P., Kent, T. A., Orme-Johnson, W. H., and Münck, E. (1985) *J. Biol. Chem. 260*, 11160−11173.
28. Lindahl, P. A., Gorelick, N. J., Münck, E., and Orme-Johnson, W. H. (1987) *J. Biol. Chem. 262*, 14945−14953.
29. Hagen, W. R., Dunham, W. R., Braaksma, A., and Haaker, H. (1985) *FEBS Lett. 187*, 146−150.
30. Hagen, W. R. (1992) in *Advances in inorganic chemistry: Iron−sulfur proteins* (Cammack, R., Ed.) pp 165−223, Academic Press, Inc., San Diego.
31. Johnson, M. K., Rees, D. C., and Adams, M. W. W. (1996) *Chem. Rev. 96*, 2817−2839.
32. Hille, R. (1996) *Chem. Rev. 96*, 2757−2816.
33. Hille, R. (1999) *Essays Biochem. 34*, 125−137.
34. Almendra, M. J., Brondino, C. D., Gavel, O., Pereira, A. S., Tavares, P., Bursakov, S., Duarte, R., Caldeira, J., Moura, J. J., and Moura, I. (1999) *Biochemistry 38*, 16366−16372.
35. Schindelin, H., Kisker, C., Schlessman, J. L., Howard, J. B., and Rees, D. C. (1997) *Nature 387*, 370−376.
36. Zumft, W. G., Mortenson, L. E., and Palmer, G. (1974) *Eur. J. Biochem. 46*, 525−535.
37. Tanaka, M., Haniu, M., Matsueda, G., Yasunobu, K. T., Mayhew, S., and Massey, V. (1971) *Biochemistry 10*, 3041−3046.
38. Tanaka, M., Haniu, M., Yasunobu, K. T., Mayhew, S., and Massey, V. (1973) *J. Biol. Chem. 248*, 4354−4366.
39. Tanaka, M., Haniu, M., Yasunobu, K. T., Mayhew, S. G., and Massey, V. (1974) *J. Biol. Chem. 249*, 4397.
40. Tanaka, M., Haniu, M., Yasunobu, K. T., and Mayhew, S. G. (1974) *J. Biol. Chem. 249*, 4393−4396.
41. Dubourdieu, M., Le Gall, J., and Fox, J. L. (1973) *Biochem. Biophys. Res. Commun. 52*, 1418−1425.

BI020033M